Developmental Cell
Article

A Gβγ Effector, ElmoE, Transduces GPCR Signaling to the Actin Network during Chemotaxis

Jianshe Yan,[1] Vassil Mihaylov,[3] Xuehua Xu,[1] Joseph A. Brzostowski,[2] Hongyan Li,[1] Lunhua Liu,[3] Timothy D. Veenstra,[4] Carole A. Parent,[3] and Tian Jin[1,*]
[1]Chemotaxis Signal Section
[2]Laboratory of Immunogenetics Imaging Facility
National Institute of Allergy and Infectious Diseases, National Institutes of Health, Rockville, MD 20852, USA
[3]Laboratory of Cellular and Molecular Biology, Center for Cancer Research, National Cancer Institute, Bethesda, MD 20892, USA
[4]Laboratory of Proteomics and Analytical Technologies, Advanced Technology Program, SAIC-Frederick, National Cancer Institute at Frederick, Frederick, MD 21702, USA
*Correspondence: tjin@niaid.nih.gov
DOI 10.1016/j.devcel.2011.11.007

SUMMARY

Activation of G protein-coupled receptors (GPCRs) leads to the dissociation of heterotrimeric G-proteins into Gα and Gβγ subunits, which go on to regulate various effectors involved in a panoply of cellular responses. During chemotaxis, Gβγ subunits regulate actin assembly and migration, but the protein(s) linking Gβγ to the actin cytoskeleton remains unknown. Here, we identified a Gβγ effector, ElmoE in *Dictyostelium*, and demonstrated that it is required for GPCR-mediated chemotaxis. Remarkably, ElmoE associates with Gβγ and Dock-like proteins to activate the small GTPase Rac, in a GPCR-dependent manner, and also associates with Arp2/3 complex and F-actin. Thus, ElmoE serves as a link between chemoattractant GPCRs, G-proteins and the actin cytoskeleton. The pathway, consisting of GPCR, Gβγ, Elmo/Dock, Rac, and Arp2/3, spatially guides the growth of dendritic actin networks in pseudopods of eukaryotic cells during chemotaxis.

INTRODUCTION

G protein-coupled receptors (GPCRs) regulate many physiological responses to hormones, neurotransmitters, chemokines and other stimuli (Dupré et al., 2009). The chemokine GPCRs detect extracellular chemical gradients to guide directional movement of eukaryotic cells toward the chemical source in a process known as chemotaxis (Jin et al., 2008; Van Haastert and Devreotes, 2004). Activation of chemokine GPCRs promotes the dissociation of the heterotrimeric G proteins Gα and Gβγ, which, in turn, activate downstream signal transduction pathways that ultimately regulate the spatiotemporal organization of the actin cytoskeleton to drive cell migration (Dong et al., 2005; Jin et al., 2008; Li et al., 2003; Van Haastert and Devreotes, 2004). Downstream pathways that control the actin network during migration have been identified. At the leading edge, Arp2/3 complexes initiate the formation of new actin filaments, branching from existing ones. The growth of the dendritic actin-network pushes the membrane forward, resulting in pseudopod extension (Insall and Machesky, 2009; Pollard and Borisy, 2003). The dominant leading front is supported through the suppression of errant pseudopods at the sides and rear of the cell by action of the cortical actin/myosin II network (Bosgraaf and van Haastert, 2006; Isik et al., 2008). In neutrophils, chemokines activate Rac1 and Rac2 to induce the growth of actin-filaments by removing capping proteins and stimulating the Arp2/3 complex, respectively (Sun et al., 2007). GPCR-induced Rac activation requires guanine nucleotide exchange factors (GEFs) (Côté and Vuori, 2007; Dong et al., 2005), one being the evolutionarily conserved Elmo/Dock180 complex (Brugnera et al., 2002; Côté and Vuori, 2007; Reddien and Horvitz, 2004), which functions to regulate chemotaxis (Côté et al., 2005). However, it is not known how Rac-GEF proteins link GPCR signaling through the heterotrimeric G protein subunits to direct the dynamic organization of the actin network during chemotaxis.

Dictyostelium discoideum is a well established model system for studying eukaryotic chemotaxis (Jin et al., 2008; Van Haastert and Devreotes, 2004). This organism utilizes the GPCR cAMP receptor 1 (cAR1) coupled with the heterotrimeric G protein Gα2Gβγ to detect the chemoattractant cAMP and control cell migration (Kimmel and Parent, 2003; Parent and Devreotes, 1999). Mechanisms of cAMP gradient sensing by cAR1/Gα2Gβγ have been studied extensively (Janetopoulos et al., 2001; Jin et al., 2000; Xu et al., 2010). Many components that regulate or constitute the actin-based moving apparatus for chemotaxis have been identified. The cAR1/Gα2Gβγ machinery activates Ras proteins that regulate four signaling enzymes, PI3K, TORC2, PLA2, and sGC, each of which has been implicated in chemotaxis (Cai et al., 2010; Charest et al., 2010; Funamoto et al., 2002; Iijima and Devreotes, 2002; Veltman et al., 2008). Despite much progress, our understanding on the signaling network controlling chemotaxis by GPCRs remains incomplete. It is still unclear which proteins interact with G protein subunits leading to activation of these enzymes, and how these enzymes control the actin cytoskeleton. The Elmo and Dock proteins are evolutionarily conserved in *D. discoideum* and likely serve as GEFs for Rac proteins controlling actin cytoskeleton in chemotaxis (Brzostowski et al., 2009a). Indeed, It has been shown that in *D. discoideum* Dock and Rac proteins regulate the actin

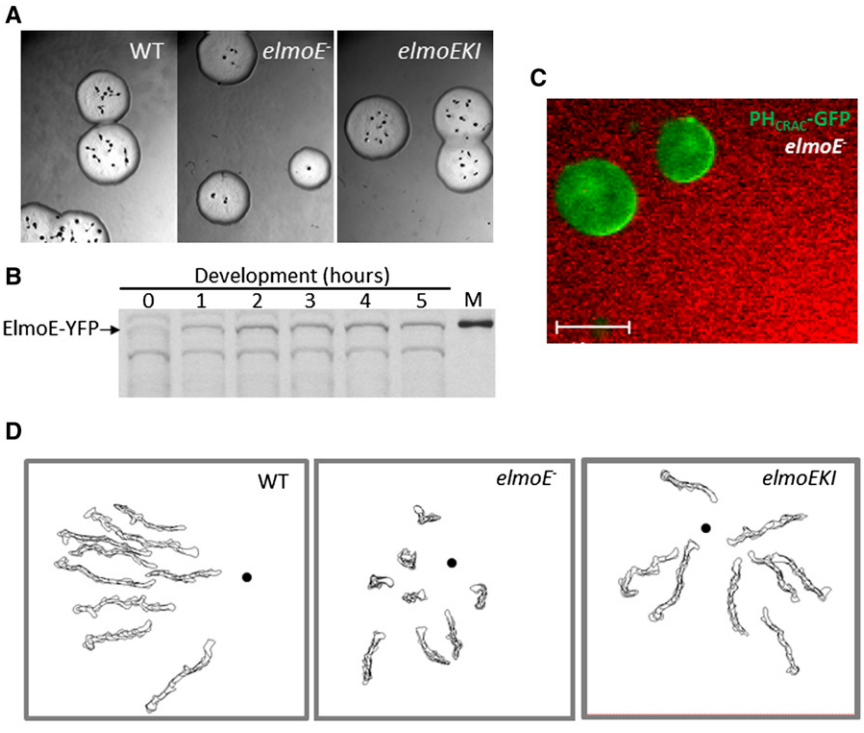

E

Cell line	Directionality	Speed (μm/min)	Direction Change	Roundness (%)
WT	0.86 +/- 0.04	10.75 +/- 1.85	20.25 +/- 4.49	48.98 +/- 5.38
elmoE-	0.56 +/- 0.18	4.94 +/- 1.14	38.49 +/- 12.28	62.81 +/- 8.93
elmoEKI	0.81 +/- 0.08	9.13 +/- 1.03	21.93 +/- 5.77	49.52 +/- 4.48

Figure 1. ElmoE Is Not Required for cAMP Gradient Sensing but Is Required for Chemotaxis

(A) *elmoE*$^-$ cells form less fruiting bodies when developed on bacterial lawns. *elmoEKI* cells have a phenotype similar to WT cells indicating that ElmoE-YFP functions normally. WT, *elmoE*$^-$, and *elmoEKI* cells were plated on nutrient agar plates with *Klebsiella aerogenes* and photographs were taken after 5 days. See also Figure S1.

(B) ElmoE protein is expressed at the chemotactic competent stage. *elmoEKI* cells were developed in suspension with exogenous cAMP pulses and the level of ElmoE-YFP was determined from 0 to 5 hr by western blot analysis using an anti-GFP antibody.

(C) Similar to wild-type cells, *elmoE*$^-$ cells are able to polarize PH_{CRAC}-GFP (green) in response to a cAMP gradient (red). Cells were treated with Latrunculin B to depolarize the actin cytoskeleton.

(D) Cell shape analysis of wild-type, *elmoE*$^-$, and *elmoEKI* migrating to a micropipette filled with 1 μM cAMP (black dots show the position of the micropipette).

(E) Chemotaxis behaviors measured by four parameters: directionality (0 represents random movement and 1 represents movement in a straight line to the micropipette); speed is defined as the distance that a cell's centroid moves as a function of time; direction change is represented by the frequency of turns the cell makes during the migration process (a higher value represents more turns, and thus inefficient chemotaxis); and roundness is an indication of cell polarization (a higher value indicates a less polarization).

cytoskeleton during chemotaxis toward a cAMP source (Para et al., 2009; Park et al., 2004), but how the cAR1/Gα2Gβγ link to downstream components to control the actin-based moving apparatus is not known.

Here, we identified ElmoE (DDB_G0279657 in dictyBase) as an essential component for cAR1-controlled chemotaxis, and importantly, we demonstrated that ElmoE associates with Gβγ subunits and interacts with Dock-like proteins to activate RacB and promote actin polymerization at the leading front of migrating cells.

RESULTS

ElmoE Plays a Role in cAR1-Mediated Chemotaxis

To examine the function of ElmoE, we generated both an *elmoE* null (*elmoE*$^-$) and an *ElmoE-YFP* knockin strain (*elmoEKI*), in which the YFP coding sequence was inserted at the 3′ end of the ElmoE gene, through homologous recombination (Figure S1 available online). *elmoE*$^-$ mutants displayed an abnormal developmental phenotype characterized by the relatively low number of fruiting bodies formed when cells are developed on a lawn of *Klebsiella aerogenes* (Figure 1A). In similar experiments, *elmoEKI* cells did not show the developmental defect, demonstrating that the ElmoE-YFP protein is functional (Figure 1A). In addition, ElmoE-YFP protein was hardly detected in vegetative *elmoEKI* cells but was expressed during the chemotaxis-competent stage, consistent with a role in chemotaxis (Figure 1B).

Chemotaxis is the result of three basic cell processes: chemoattractant gradient sensing, actin-dependent cell polarization, and actin-mediated cell motility (Iijima et al., 2002). To test whether ElmoE plays a role in gradient sensing, we examined chemoattractant-induced polarization of PIP_3 on the plasma membrane in cells exposed to a gradient of chemoattractant. Polarization of PIP_3 is regulated by cAR1/Gα2βγ and requires inputs from Ras, PI3K, and PTEN (Funamoto et al., 2002; Iijima and Devreotes, 2002). Changes in the level of PIP_3 were monitored in vivo by the PIP_3-binding fluorescent probe PH_{CRAC}-GFP (Parent et al., 1998). We found that in both *elmoE*$^-$ and wild-type cells (Xu et al., 2005) PH_{CRAC}-GFP localized similarly toward a chemoattractant gradient emanating from a point source (Figure 1C), indicating that ElmoE is not essential for gradient sensing. However, *elmoE*$^-$ cells showed a clear defect in directional cell migration. We recorded cell movement toward a chemoattractant gradient (Figure 1D) and determined four chemotactic parameters for wild-type, *elmoE*$^-$, and *elmoEKI* cells (Figure 1E). Our analyses showed that *elmoE*$^-$ cells exhibited significantly poorer directionality, lower speed, more direction changes, and reduced polarization (higher value of roundness) compared to wild-type or *elmoEKI* cells. These results indicate that ElmoE plays a role in cAR1/Gα2βγ-mediated

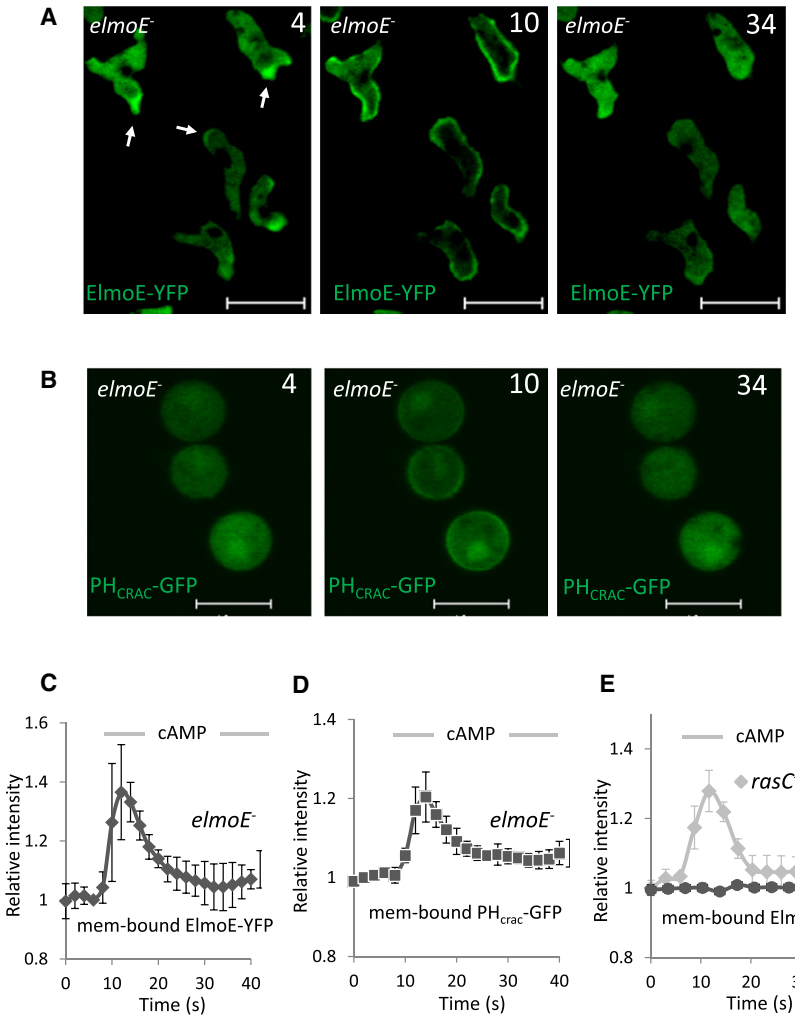

Figure 2. ElmoE-YFP and PH_{CRAC}-GFP Translocation Kinetics

(A and C) ElmoE-YFP transiently associates with plasma membrane upon cAMP stimulation. *elmoE*$^-$ cells expressing ElmoE-YFP were stimulated with cAMP at 6 s. Images were captured at 2 s intervals and frames in the YFP channel at selected time points are shown. The kinetics of the time course is graphed in (C).

(B and D) cAMP-induced PH_{CRAC}-GFP translocation appears normal in *elmoE*$^-$ cells. *elmoE*$^-$ cells expressing PH_{CRAC}-GFP were treated with Latrunculin B to depolarize the actin cytoskeleton and stimulated with cAMP at 6 s.

(E) cAMP-induced ElmoE membrane translocation requires cAR1/G protein signaling but does not require RasC or RasG. Temporal changes in the levels of ElmoE-YFP at the plasma membrane are shown as a time course for *gβ*$^-$ cells expressing ElmoE-YFP and *rasC*$^-$*&rasG*$^-$ cells expressing ElmoE-YFP. The transient fluorescence intensity increase was measured at the plasma membrane and graphed. Mean (n = 6) and standard deviation (SD) are shown for the time course. See also Figure S2.

chemotaxis, affecting both cell polarization and motility, two processes that require the actin-cytoskeleton.

ElmoE Translocates to the Cell Membrane upon Activation of cAR1/Gα2βγ

Activation of cAR1 GPCR induces dissociation of heterotrimeric G-proteins into Gα2 and Gβγ subunits, which regulate multiple signal transduction pathways controlling the actin-cytoskeleton that drives cell migration (Iijima et al., 2002; Jin et al., 2008; Van Haastert and Devreotes, 2004). We first observed the cellular localization of ElmoE-YFP upon a uniform cAMP stimulation (Figure 2A). Before the stimulation, ElmoE was enriched at the leading front and was also distributed in cytosol of chemotaxing cells. Stimulation triggered a transient translocation of ElmoE-YFP to the plasma membrane (Figures 2A and 2C), indicating that activation of cAR1/Gα2βγ mediates cellular localization of ElmoE. When cells were treated with Latrunculin B, which destroys the actin cytoskeleton, cAMP-stimulation did not induce a clear membrane translocation of ElmoE-YFP (data not shown), suggesting that cAMP-induced membrane translocation of ElmoE depends on the actin cytoskeleton.

It has been shown that cAR1/Gα2βγ activates the small G-proteins RasC and RasG to control TORC2 and PI3K activities respectively, and each of which in turn transduces signals to the actin-cytoskeleton (Cai et al., 2010; Charest et al., 2010; Iijima and Devreotes, 2002; Veltman et al., 2008). To understand the role of each pathway in cAR1-mediated ElmoE membrane translocation, we examined ElmoE-YFP cellular distribution in the cells that had been treated with LY, which blocks PI3K, and in *pia*$^-$ cells, in which there is no functional TORC2 complex (Chen et al., 1997) (Figure S2). Furthermore, we monitored ElmoE-YFP distribution in cells lacking RasC and RasG, *rasC*$^-$/*rasG*$^-$, or a functional heterotrimeric G protein complex, *gβ*$^-$ (Wu et al., 1995) (Figure 2E; Figure S2). With the exception of *gβ*$^-$ cells, we observed a clear cAMP-induced membrane translocation of ElmoE-YFP under all conditions (Figure 2E; Figure S2). Furthermore, consistent with our gradient experiments (see Figure 1C), the cAR1-induced PIP_3 response to cAMP stimulation was normal in *elmoE*$^-$ cells as monitored by the transient translocation of PH_{CRAC}-GFP to the plasma membrane (Figures 2B and 2D). Thus, the plasma membrane translocation of ElmoE is mediated by heterotrimeric G-proteins and requires the actin-cytoskeleton, but does not require RasC, RasG, PI3K, and TORC2.

Proteomic Analyses Suggest that ElmoE Associates with Gβγ, RacB, and the Arp2/3 complex

To reveal the potential molecular mechanism of ElmoE function, we sought to identify proteins that associate with ElmoE (Figure 3). ElmoE-YFP-TAP expressed in *elmoE*$^-$ cells was partially purified from lysates using anti-GFP antibodies coupled to

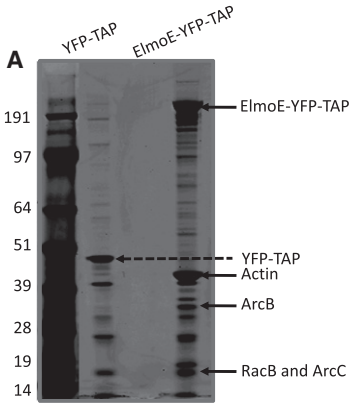

B

Gβ	trimeric G-protein
RacB	small G-protein
ArcA	Arp2/3 complex
ArcB	
ArcC	
ArcD	
ArcE	
ArpB	
ArpC	
act22	actin
act16	

C

	His-S-HA-Gβ		His-HA-CRAC	
	Count Peptds	Diffrnt Peptds	Count Peptds	Diffrnt Piptds
ElmoE	13	10	0	0
Gγ	29	8	0	0
Gα4	8	7	0	0
GbqA	7	3	0	0
Gα2	3	3	0	0

Figure 3. ElmoE Forms Complex with Gβγ, RacB, the Arp2/3 Complex, and Actin

(A) Lysates of *elmoE*$^{-}$ cells expressing ElmoE-YFP-TAP (E-Y-T) or YFP-TAP (Y-T; as a control) were incubated with beads coupled with anti-GFP antibodies. Elutes were subjected to SDS gel electrophoresis and stained with Coomassie blue. Selected bands were excised from the gel and identified using mass spectrometry.

(B) Proteins identified by mass spectrometry that associate with ElmoE are shown. See also Figure S3A and Table S1.

(C) Proteins crosslinked to His-S-HA-Gβ by HBVS as determined by mass spectrometry are shown. The numbers of peptides determined by mass spectrometry are listed for both control (His-S-HA-CRAC) and His-S-HA-Gβ. Count Peptides: the total number of peptides that were identified for a specific protein (includes peptides that were observed more than once); Different Peptides: the number of unique peptides that were identified for a specific protein. See also Figure S3.

beads, and eluates were subjected to SDS gel electrophoresis; the YFP-TAP tag expressed in cells was used as a control. Several prominent protein bands, which appeared specifically in the ElmoE-YFP-TAP but not in the control sample, were identified using mass spectrometry (Figure 3A). The identified proteins include RacB, ArcB, and ArcC (components in the Arp2/3 complex), as well as actin (act22 and act16 in dictyBase). We then applied a comprehensive proteomic analysis to identify all proteins that immunoprecipitated with ElmoE-YFP-TAP but not the YFP-TAP tag (Figure S3A; Table S1). The analysis confirmed that RacB, ArcB, and ArcC as well as act22 and act16 coimmunoprecipitated with ElmoE-YFP-TAP. We also discovered that the Gβ subunit of the heterotrimeric G protein and other components of the Arp2/3 complex associated with ElmoE-YFP-TAP but not the YFP-TAP (Figure 3B; Table S1).

To further examine the interaction between Gβγ and ElmoE, we identified proteins that associate with Gβ subunit using a proteomic approach. Cells expressing His-S-HA-Gβ or His-S-HA-CRAC (Insall et al., 1994) (as a control) were stimulated with cAMP. HBVS was added to cell lysates to chemically crosslink proteins. The crosslinked lysates were precleared by centrifugation, and the supernatant was then subjected to tandem affinity purification with Ni-NTA agarose and S-protein agarose. The eluted protein complexes were subjected to mass spectrometry. We found that ElmoE, Gγ, Gα4, GbqA (a Gα subunit), and Gα2 crosslinked to His-S-HA-Gβ but not to the His-S-HA-CRAC control (Figure 3C). Identification of Gγ and Gαs, which are known to interact with Gβ to form a heterotrimeric complex (Hadwiger and Firtel, 1992; Janetopoulos et al., 2001; Zhang et al., 2001), indicated that this approach successfully revealed Gβ associating proteins, including that identified here, ElmoE. Because HBVS crosslinks proteins at distances less than 15 Å (Figure S3), our data suggest that ElmoE interacts with Gβγ.

Gβγ Associates with ElmoE

The association between Gβ and ElmoE was further confirmed by immunoprecipitation analyses. In pull-downs of lysates from cells expressing ElmoE-YFP using an anti-GFP antibody, we found that native Gβ coimmunoprecipitated with ElmoE-YFP (Figure 4A). In reciprocal experiments, lysates from cells coexpressing ElmoE-YFP and His-S-HA-Gβ or ElmoE-YFP and His-S-HA-CRAC or His-S-HA-PH_{CRAC}, as controls, were immunoprecipitated to with anti-HA antibody. ElmoE-YFP coimmunoprecipitated with His-S-HA-Gβ but not His-S-HA-CRAC or His-S-HA-PH_{CRAC} (Figure 4B).

To understand how Gβ and ElmoE may associate, we performed coimmunoprecipitation analyses on extracts from cells coexpressing ElmoE-YFP and mutant Gβ subunits designated SN (Jin et al., 1998). GβSN point mutants were previously isolated as a class of Gβ mutants that specifically fail to activate the adenylyl cyclase but retain the ability to carry out cAMP-induced actin polymerization (Jin et al., 1998). We found that ElmoE-YFP coimmunoprecipitated with GST-tagged GβSN1, GβSN2 and GβSN8 but not the GST-tag control (Figure 4C), indicating that the residues needed for adenylyl cyclase activation are not required for association with ElmoE. These results are consistent with the notion that association between Gβγ and ElmoE does not involve signaling proteins that function to activate adenylyl cyclase, such as, RasC and G, PI3K, or TORC2.

To further understand the ElmoE-Gβ interaction, we generated two ElmoE deletion mutants and assessed their ability to associate with Gβ and translocate to the plasma membrane after a cAMP stimulation (Figures 4D and 4E). N-ElmoE-YFP consists of the first 1044 amino acids of ElmoE, which includes the Elmo domain (Brzostowski et al., 2009b). C-ElmoE-YFP consists of the second half of ElmoE (from 1039 aa to 1668 aa), which contains a coiled-coil domain. Immunoprecipitation analyses showed that N-ElmoE-YFP associated with Gβ while C-ElmoE-YFP did not. As an additional control, we found that Gβ does not coimmunoprecipitate with ElmoA-GFP (Figure 4E), another *D. discoideum* Elmo family protein (Isik et al., 2008). These results indicate that Gβ specifically associates with the N-terminal portion of ElmoE. Interestingly, cAMP stimulation induced a clear membrane translocation of C-ElmoE-YFP (Figure 4F) but not N-ElmoE-YFP (data not shown). In addition, the translocation exhibited by the C-ElmoE-YFP did not occur when cells were treated with Latrunculin B, similar to that exhibited by full-length ElmoE-YFP (Figure 4F). Taken together, our results suggest that ElmoE receives two kinds of signals from the cAR1/Gα2βγ

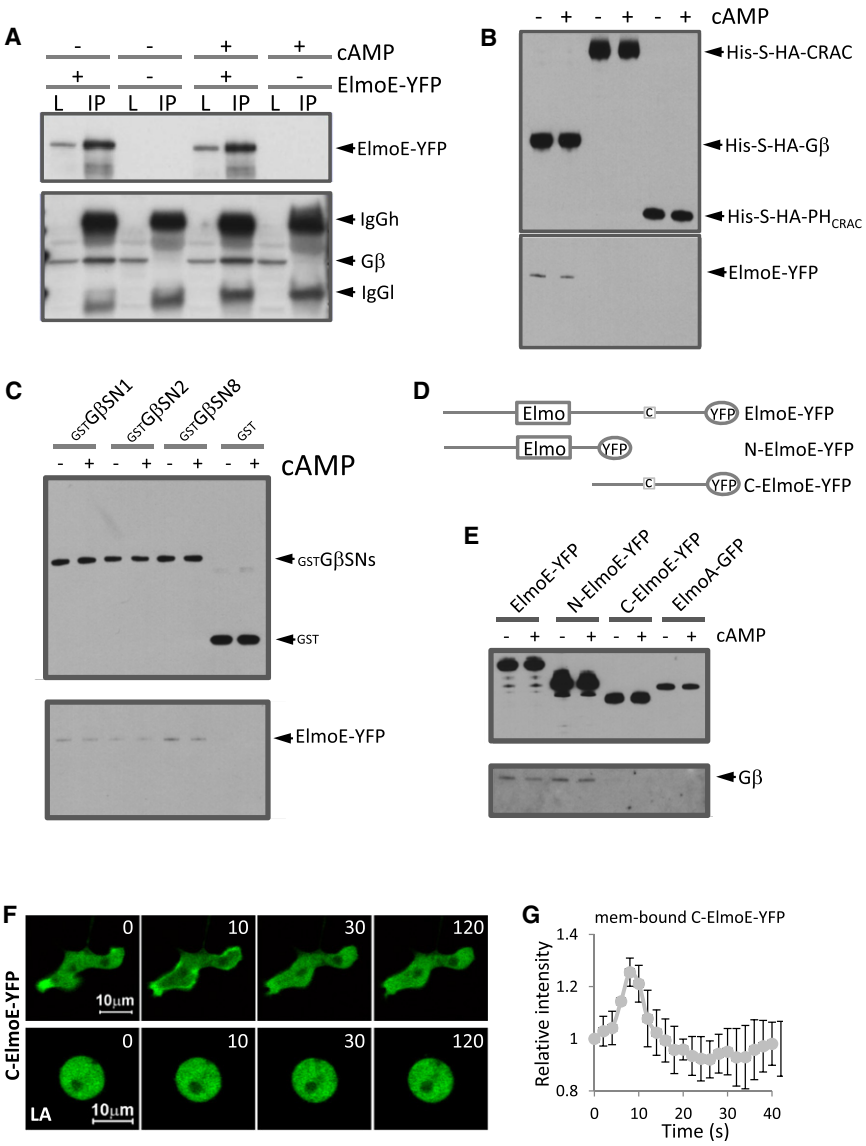

Figure 4. The Association between Gβγ and ElmoE

(A) Lysates of WT (negative control) or *elmoE*$^-$ cells expressing ElmoE-YFP (– or + ElmoE-YFP, respectively), which were stimulated with 0 or 50 μM cAMP (– or + cAMP), were incubated with anti-GFP beads, and elutes analyzed by immunoblotting to detect Gβ. About 1% lysates was applied on lanes L and 19% of lysates was applied on lanes IP.

(B) Lysates of ElmoE$^-$ cells coexpressing ElmoE-YFP and His-S-HA-Gβ, His-S-HA-CRAC, or His-S-HA-PH_{CRAC} were stimulated with 0 or 10 μM cAMP (– or + cAMP), were incubated with beads coupled with anti-HA antibodies and elutes were analyzed by immunoblotting using anti-GFP antibodies to detect ElmoE-YFP. See also Figure S4.

(C) Cells of *ElmoE*$^-$ cells coexpressing ElmoE-YFP and GST (as a control) or GST-GβSN1, GST-GβSN2, and GST-GβSN8 were stimulated with 0 or 10 μM cAMP (– or + cAMP). Lysates were incubated with beads coupled with anti-GST antibodies and elutes were analyzed by immunoblotting using anti-GFP antibodies to detect ElmoE-YFP.

(D) YFP tagged ElmoE and two deletion mutants were generated as indicated. N-ElmoE-YFP consists of the N-terminal portion of ElmoE (from 1 aa to 1044 aa), which includes the Elmo domain. C-ElmoE-YFP consists of the C-terminal portion of ElmoE (from 1039 aa to 1668 aa), which contains a coiled-coil domain.

(E) *ElmoE*$^-$ cells expressing ElmoE-YFP, N-ElmoE-YFP, C-ElmoE-YFP, and ElmoA-GFP (as a control) were stimulated with 0 or 10 μM cAMP (– or + cAMP). Lysates were incubated with beads coupled with anti-GFP antibodies and elutes were analyzed by immunoblotting to detect Gβ.

(F and G) C-ElmoE-YFP transiently associates with plasma membrane upon cAMP stimulation. *elmoE*$^-$ cells expressing C-ElmoE-YFP were stimulated with cAMP. Images were captured at 2 s intervals and frames in the YFP channel at selected time points are shown. The kinetics of the time course is graphed in (G). Means (n = 6) and SDs are shown.

machinery: one from Gβγ to its N-terminal portion, and the other, a potential feedback signal, to its C-terminal portion from the actin cytoskeleton.

ElmoE Associates with Dock-Like Proteins and RacB

Eight genes have been found to encode Dock-like proteins in *D. discoideum* (Meller et al., 2005). Among them, DdDockA, B, C, and D belong to the subfamily of Dock180-related proteins, and DdzizA, B, C, and D belong to the subfamily of zizimin-related proteins, which include mammalian Dock9 and 10 (Meller et al., 2005). To determine which of the Dock family proteins associate with ElmoE, Dock-like proteins were epitope-tagged, expressed in cells with ElmoE-YFP and coimmunoprecipitation analyses were performed (Figures 5A and 5B; note that DdDockA was not examined because we were not able to coexpress GST-DdDockA). We found that ElmoE-YFP coimmunoprecipitated with GST tagged DdDockC and DdzizA but not any other family member (Figures 5A and 5B; Figure S4).

The association between ElmoE and RacB was confirmed by immunoprecipitation analyses (Figures 5C and 5D). Lysates of cells coexpressing myc-tagged RacB and ElmoE-YFP or PH_{CRAC}-GFP (as a control) were immunoprecipitated using anti-GFP antibodies coupled to beads, elutes were subjected immunoblot analysis using anti-myc antibody (Figure 5C). We found that myc-RacB coimmunoprecipitated with ElmoE-YFP but not PH_{CRAC}-GFP. In a reciprocal experiment, ElmoE-YFP but not PH_{CRAC}-GFP coimmunoprecipitated with myc-RacB. Our results suggest that ElmoE and DdDockC and (or) DdzizA form the evolutionarily conserved Elmo/Dock complex that likely serves as the GEF(s) for the small G protein RacB.

Activation of cAR1 Promotes Association between Gβγ and ElmoE

To evaluate how activation of cAR1 affects the association between Gβ and ElmoE, we performed coimmunoprecipitation analyses on the membrane fraction from cells coexpressing

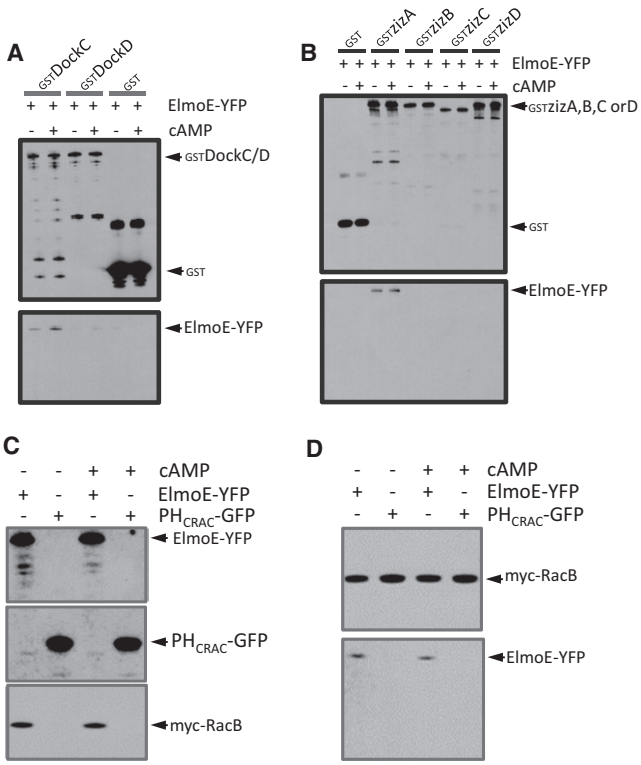

Figure 5. ElmoE Associates with Dock-like Proteins and RacB

(A and B) *ElmoE*$^-$ cells coexpressing ElmoE-YFP and GST tagged Dock-like proteins or GST tag (as a control) were stimulated with 0 or 10 μM cAMP (− or + cAMP). Lysates were incubated with beads coupled with anti-GST antibodies and elutes were analyzed by immunoblotting using anti-GFP antibodies to detect ElmoE-YFP.

(C) Cells coexpressing myc-RacB and ElmoE-YFP (+ ElmoE-YFP) or PH_{CRAC}-GFP (+ PH_{CRAC}-GFP, control) were stimulated with 0 or 10 μM cAMP (− or + cAMP). Cell lysates were incubated with beads coupled with anti-GFP and elutes were analyzed by immunoblotting to detect myc tagged RacB.

(D) Cells coexpressing myc-RacB with ElmoE-YFP (+ ElmoE-YFP) or PH_{CRAC}-GFP (+ PH_{CRAC}-GFP, control) were stimulated with 0 or 10 μM cAMP (− or + cAMP). Cell lysates were incubated with beads coupled with anti-myc antibodies and elutes were analyzed by immunoblotting using an anti-GFP antibody. See also Figure S5.

His-S-HA-tagged Gβ and ElmoE-YFP, N-ElmoE-YFP, or C-ElmoE-YFP (Figures 6A and 6B). After cells were stimulated with 10 μM cAMP, membrane fractions were isolated at various time points and immunoprecipitated using the HA antibody coupled to beads to pull down His-S-HA-Gβ. To determine the amount of ElmoE-YFP, N-Elmo-YFP, and C-Elmo-YFP that associates with His-S-HA-Gβ upon cAMP stimulation, elutes at various time points were subjected to western blot analysis using the anti-GFP antibody (Figures 6A and 6B). We found that cAMP stimulation induced a clear increase in the level of ElmoE-YFP associating with His-S-HA-Gβ (Figures 6A and 6C). In contrast, N-ElmoE-YFP associated with His-S-HA-Gβ but the level of N-ElmoE-YFP remained unchanged upon a cAMP stimulation (Figures 6B and 6C), while C-ElmoE-YFP that translocates to membrane upon a cAMP stimulation did not associate with Gβ (Figure 6B).

We further examined dynamics of Gβγ/ElmoE association upon uniform cAMP stimulation in single live cells using a sensitized emission FRET imaging method (Brzostowski et al., 2009b). Cells coexpressing Gβ-CFP/ElmoE-YFP or cAR1-CFP/ElmoE-YFP (as a control) were imaged in three channels (CFP, FRET, and YFP) over a time lapse after cAMP stimulation (Figure S6). As predicted, the normalized FRET (N-FRET) between cAR1-CFP and ElmoE-YFP remained low and unchanged following cAMP addition (Figure 6D). In contrast, a sharp increase in N-FRET between Gβ-CFP and ElmoE-YFP was measured upon cAMP stimulation concurrent with ElmoE-YFP translocation to the plasma membrane (Figure 6E). Interestingly, the N-FRET signal remained high even after the bulk of the ElmoE-YFP signal returned to the cytosol (Figure 6E), consistent with previous findings that Gβγ remains dissociated from Gα under persistent stimulatory conditions (Janetopoulos et al., 2001; Xu et al., 2005, 2007).

Taken together, our data indicate that activation of cAR1 promotes the association of Gβγ and ElmoE. N-terminal region of ElmoE (the first 1044 aa) interacts with Gβ, while C-terminal region of ElmoE (from 1039 aa to 1668 aa) facilitates membrane translocation of ElmoE. Before a cAMP stimulation, there is a basal level of association between Gβγ and ElmoE. Our observation that ElmoE localizes at the leading front of chemotaxing cells before a cAMP stimulation (Figure 2A) is consistent with the notion that ElmoE associates with Gβγ at the leading front of polarized cells in the absence of cAMP. cAMP stimulation promotes the association between Gβγ and ElmoE by generating more free Gβγ subunits on the membrane and recruiting more ElmoE to the membrane.

Gβγ-ElmoE Association and Membrane Translocation of ElmoE Are Required for Proper Chemotaxis

To test whether the Gβγ-ElmoE association and/or cAMP-induced membrane translocation are crucial for ElmoE functions, we examined developmental phenotype and chemotaxis of *elmoE*$^-$ cells expressing N-ElmoE-YFP and C-ElmoE-YFP. As shown previously (Figure 1A), *elmoE*$^-$ cells displayed a developmental phenotype. Expressing ElmoE-YFP rescued the phenotype. In contrast, expressing either N-ElmoE-YFP or C-ElmoE-YFP in *elmoE*$^-$ cells did not rescue the developmental phenotype (Figure S6). Using a TAXIScan assay, we examined chemotaxic behaviors of wild-type, *elmoE*$^-$, and *elmoE*$^-$ cells expressing ElmoE-YFP, N-ElmoE-YFP, or C-ElmoE-YFP toward a linear cAMP gradient (0 μM–0.5 μM) (Figures 6F and 6G; Figure S6). The *elmoE*$^-$ cells displayed significant defects in chemotaxis index and speed, while *elmoE*$^-$ cells expressing ElmoE-YFP rescued the chemotaxis defects, consistent with previous results (Figure 1). In contrast, expressing either N-ElmoE-YFP or C-ElmoE-YFP did not rescue the chemotaxis defects. These results suggest that both membrane translocation and the Gβ association of ElmoE are important for normal development and chemotaxis.

ElmoE Is Required for cAR1-Triggered RacB Activation

Because RacB was found to associate with ElmoE, we next tested whether ElmoE regulates RacB activity. Upon cAMP stimulation, RacB was activated in cells expressing ElmoE but in cells lacking ElmoE or cAR1, the stimulation failed to induce RacB activation (Figures 6H and 6I). There are 18 Rac-related GTPases belonging to the Rho family and 42 proteins with a Rho-GEF

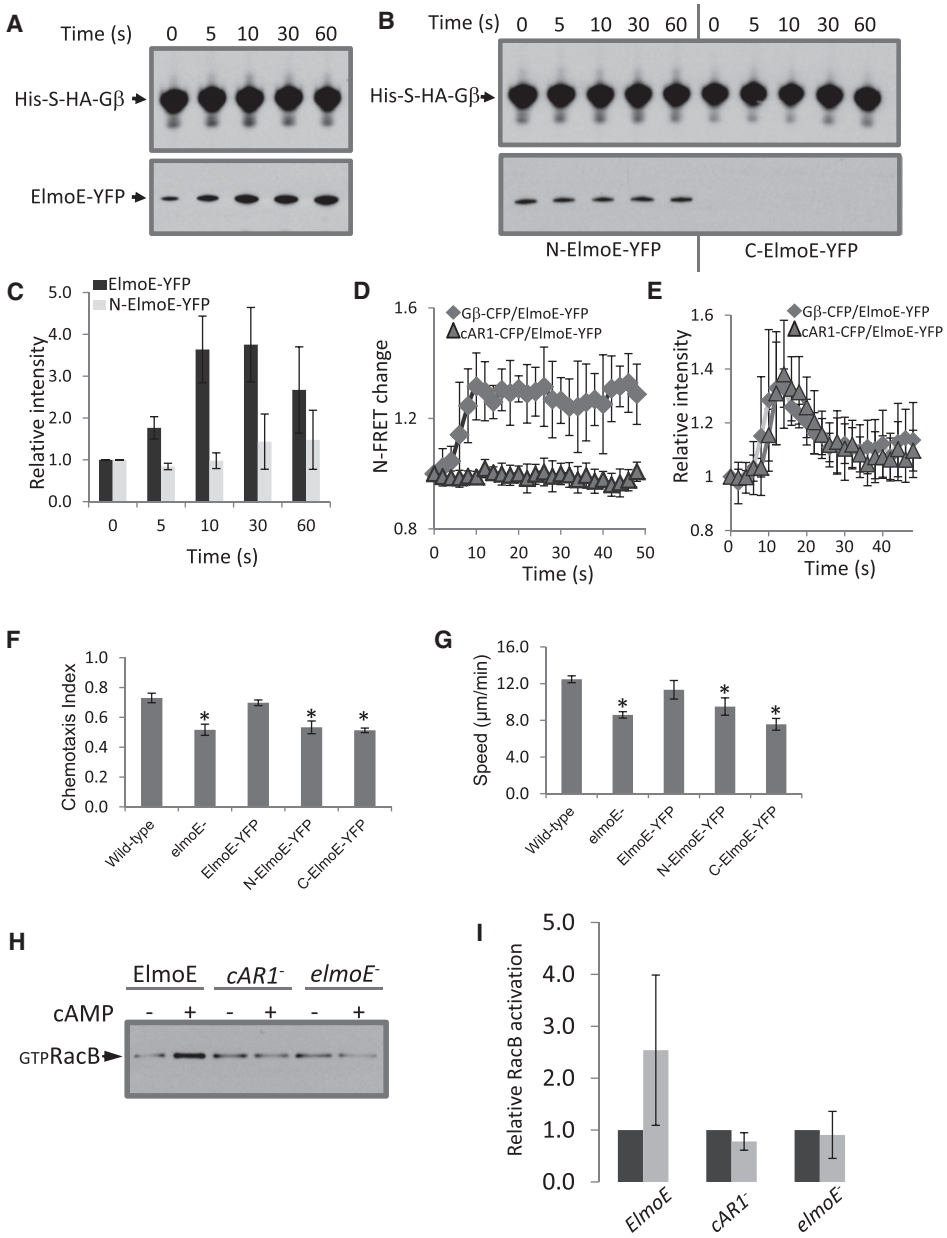

Figure 6. Activation of cAR1 Promotes the Association between Gβγ and ElmoE and Induces RacB Activation

(A–C) Activation of cAR1 promotes interaction between Gβγ and ElmoE. Cells of *ElmoE*$^-$ cells coexpressing His-S-HA-Gβ and ElmoE-YFP, N-ElmoE-YFP, or C-ElmoE-YFP were stimulated with 0 or 10 μM cAMP (− or + cAMP). Membrane fractions were collected at the indicated time points. Lysates were incubated with beads coupled with anti-HA antibodies and elutes were analyzed by immunoblotting with anti-GFP to detect ElmoE-YFP, N-ElmoE-YFP, and C-ElmoE-YFP. The change in the amount of immunoprecipitated proteins is graphed in C (n = 3 and SDs are shown; ~1.3% ElmoE-YFP proteins associated with Gβ at time 0).

(D) cAMP stimulation induces association between ElmoE and Gβγ. Cells expressing Gβ-CFP/ElmoE-YFP or cAR1-CFP/ElmoE-YFP (control) were stimulated at 4 s. Images over a time lapse were acquired using confocal microscopy. The change in N-FRET for Gβ-CFP/ElmoE-YFP (diamond) and cAR1-CFP/ElmoE-YFP (triangle) over time as a mean and SD (n = 7 and 8, respectively) are shown. At time 0 N-FRET value for cAR1-CFP/ElmoE-YFP is 0.1036 (SD = 0.0132, n = 14), and the value for Gβ-CFP/ElmoE-YFP is 0.1620 (SD = 0.027, n = 16). See also Figure S6.

(E) The temporal change in the level of ElmoE-YFP at the plasma membrane of cells expressing Gβ-CFP/ElmoE-YFP (diamond) and cAR1-CFP/ElmoE-YFP (triangle) are shown. Shown as mean and SD (n = 7 and 8, respectively).

(F and G) EZ-TAXIScan chemotaxis toward a linear cAMP gradient of wild-type, *ElmoE*$^-$, *ElmoE*$^-$/ElmoE-YFP, *ElmoE*$^-$/N-ElmoE-YFP, and *ElmoE*$^-$/C-ElmoE-YFP cells. Results represent the average ± SD of four independent experiments. *p < 0.01 compared to wild-type group. See also Figure S6.

(H) cAMP-induced RacB activation requires cAR1 and ElmoE. Lysates of *elmoE*$^-$ cells expressing ElmoE-YFP *car1*$^-$ or *elmoE*$^-$ cells with or without 10 μM cAMP (− or + cAMP) stimulation were incubated with GST-Sepharose beads with PAK-PBD to bind activated Rac proteins. All cell lines express myc-RacB. Activated RacB was detected by immunoblotting using an anti-myc antibody. See also Figure S6.

(I) Upon cAMP stimulation, RacB activation in *elmoE*$^-$ cells expressing ElmoE-YFP *car1*$^-$ or *elmoE*$^-$ cells is shown as a mean ± SD of seven independent experiments; all cell lines express myc-RacB.

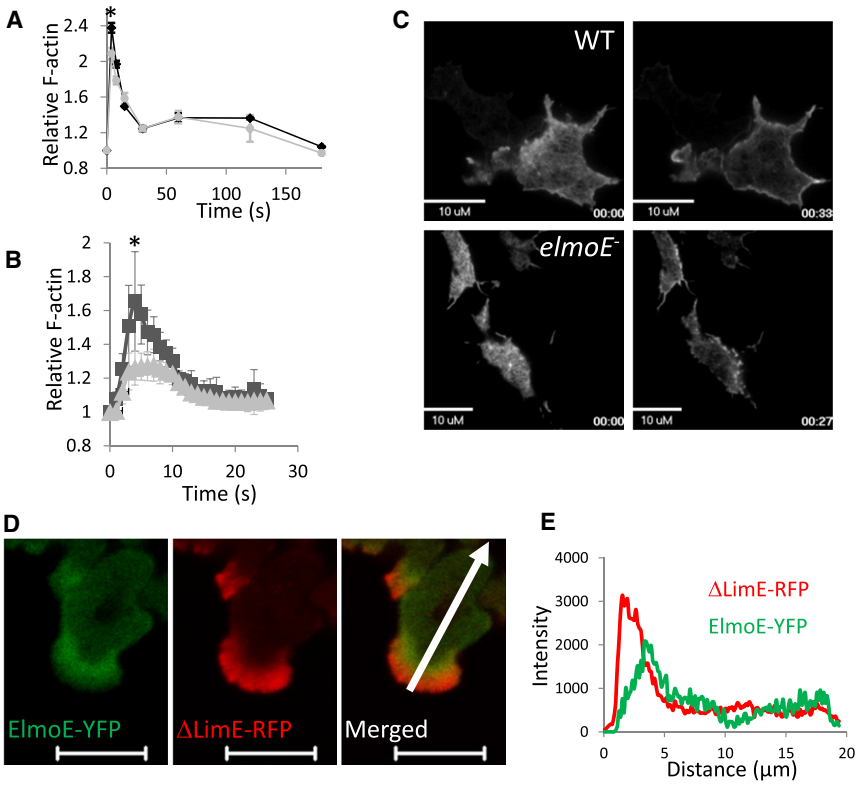

Figure 7. ElmoE Plays a Role in Actin Polymerization at the Leading Front of Chemotaxing Cells

(A) cAMP-induced actin polymerization over a time course. Wild-type and *elmoE*$^-$ cells were stimulated with a uniform stimulation of 1 μM cAMP and fixed at indicated time points. F-actin content was detected by rhodamine-phalloidin staining. Results represent the average ± SD of three independent experiments.

(B) F-actin membrane translocation. Temporal changes in the relative level of the membrane ΔLimE-RFP pool in response to a cAMP stimulation in wild-type and *elmoE*$^-$ cells is shown. Mean (n = 14) and SD are shown.

(C) Wild-type and *elmoE*$^-$ cells expressing ABD-GFP were imaged using TIR-FM.

(D) ElmoE accumulates at the leading edge of a chemotaxing cell, concentrating at the base of the growing F-actin network that drives extension of the pseudopod. Shown is a cell migrating toward a cAMP source (at bottom). See also Figure S7. The distribution of ElmoE-YFP and F-actin (ΔlimE-RFP) is shown green and red, respectively.

(E) The intensity of ElmoE-YFP and ΔlimE-RFP from the front to the back of the cell measured along the line in the merged image (D) is plotted.

(F–H) The cellular distribution of RacB, Arp2/3 complex, and ABD-GFP in chemotaxing cells using the under agar assay are shown. *Indicates the cAMP source.

domain in *D. discoideum* (Mondal et al., 2007; Vlahou and Rivero, 2006). To examine whether ElmoE is a pan regulator of Rac activity, we measured the cAMP-induced activation of two additional Rac proteins RacD and RacI in cells lacking ElmoE. In contrast to RacB, RacD and RacI were clearly activated in *elmoE*$^-$ cells (Figure S6E). Although our survey of Rac proteins was limited, these results suggest, in conjunction with our mass spec data, that ElmoE plays a role in cAR1-induced activation of RacB but not activation of all Rac proteins.

ElmoE Regulates cAMP-Induced Actin Polymerization

To reveal the relationship between ElmoE and the actin cytoskeleton, we first biochemically measured cAMP-induced actin polymerization over a time course. In wild-type cells, cAMP-induced actin polymerization is a Gα2Gβγ-dependent process that has an initial, large rapid increase in F-actin, followed by an elongated and small second peak (Cai et al., 2010; Charest et al., 2010). When *elmoE*$^-$ cells were stimulated with the same dose of cAMP, a reduced initial peak of F-actin was observed (Figure 7A). We then imaged cAMP-induced actin polymerization in live cells using an F-actin-binding probe ΔlimE-RFP by confocal microscopy (Isik et al., 2008). When cells were exposed to a uniformly applied cAMP stimulation, ΔlimE-RFP translocated to the cell cortex, indicating an increase of F-actin and then returned to cytosol in both wild-type and *elmoE*$^-$ cells (Figure 7B; Figure S7). However, the level of actin polymerization was reduced in *elmoE*$^-$ cells (Figure 7B). Interestingly, cells lacking RacB also exhibit a similar reduction in the level of cAMP-induced actin polymerization (Park et al., 2004).

To better observe the detailed structures of the actin cytoskeleton, we imaged wild-type and *elmoE*$^-$ cells expressing the fluorescent F-actin probe ABD-GFP using total internal reflection-fluorescence microscopy (Bretschneider et al., 2004) (TIR-FM). The TIR-FM imaging plane is spatially limited to ~100 nm from the coverslip and, thus, eliminates interfering, out of focus fluorescence in adherent cells. In both cell lines, the actin network underwent dynamic change even before cAMP stimulation. Upon stimulation, F-actin was transiently enriched at the cell periphery where membrane protrusions are located (Figure 7C). The transient decrease in signal at the cell's contact area with the coverslip was likely due to depletion of free ABD-GFP as it was recruited to sites of rapid actin polymerization. These events were followed by the formation of more actin filaments in the contact region and in newly forming pseudopods

(see Movie S1). We did not observe obvious defects in the initial organization or reorganization of actin network induced by chemoattractant in *elmoE*$^-$ cells by this methodology (Movie S2). Taken together, our results suggest that ElmoE is necessary for the magnitude of F-actin accumulation during the immediate "cringe" response to receptor stimulation (Futrelle et al., 1982). While the global organization of the actin network appears unaffected by the loss of ElmoE when cells experience a uniform stimulation, maintenance of polarity and directional movement are significantly compromised when cells lacking ElmoE are exposed to a chemoattractant gradient.

ElmoE Is Enriched at the Leading Pseudopod of Chemotaxing Cells

Next, we examined the cellular distribution of ElmoE, RacB, Arp2/3 complex, and the actin cytoskeleton in live cells. Cells expressing ElmoE-YFP and ΔlimE-RFP were imaged by confocal microscopy under different conditions to study how the dynamics of ElmoE localization correlates with formation of F-actin structures. In vegetative cells, ElmoE and F-actin colocalized to macropinosomes—highly dynamic F-actin-rich structures that are responsible for nutrient uptake (Figure S7A). Upon uniform cAMP stimulation of differentiated cells, both ElmoE and F-actin transiently translocated to the plasma membrane (Figures S7B and S7C). Using an under agar chemotaxis assay to ensure that cells are uniformly flat, we found that ElmoE accumulated at the base of extending F-actin filaments that drive the extension of the leading pseudopods during directional cell migration (Figures 7D and 7E). We also imaged chemotaxing cells expressing RacB-GFP and Arp2-GFP using the under agar assay. RacB-GFP, which monitors both inactive (GDP-bound) and active (GTP-bound) RacB, was uniformly distributed in cytosol of chemotaxing cells (Figure 7F), indicating that RacB proteins are accessible for activation throughout the cell. As expected, Arp2-GFP was enriched at the anterior of the cell where it organizes actin assembly in leading pseudopods to drive cell migration (Figure 7G) (Bretschneider et al., 2004). In *elmoE*$^-$ cells, the localizations of RacB and Arp2-GFP appeared normal (Figures 7F and 7G), and actin polymerization took place at the leading front of migrating cells (Figure 7H), indicating that signals are still transduced from cAR1/Gα2βγ to the actin cytoskeleton in the absent of ElmoE, which supports the idea that multiple pathways relay signals from the GPCR to the actin cytoskeleton in chemotaxis. However, the distributions of these components are consistent with the notion that ElmoE may play a role in localizing the activation of RacB at the leading front where Arp2/3 complexes are localized to promote the growth of the dendritic actin network driving cell migration.

DISCUSSION

The evidence presented here reveals a pathway in which an Elmo protein functions to link the heterotrimeric G protein Gβγ to Rac activation, ultimately regulating actin polarization in chemotaxis.

From studies in *Caenorhabditis elegans* and mammalian cells, it was established that cell surface receptors, including GPCRs, regulate Elmo/Dock complexes to activate Rac proteins to mediate pseudopod protrusion during cell migration (Côté and Vuori, 2007; Reddien and Horvitz, 2004). However, the signaling component(s) that link receptors to Elmo/Dock complexes remained unclear. Our study shows that GPCRs can regulate Elmo function via an association between Gβγ and an Elmo protein. The results of our pull-down and coimmunoprecipitation experiments indicate that the Gβ subunit associates with ElmoE and that signaling through cAR1/Gα2βγ targets two different regions of ElmoE. Specifically, Gβ associates with the N-terminal portion of ElmoE containing the Elmo domain, and cAMP-induced membrane translocation of ElmoE was shown to be mediated through the C-terminal portion of ElmoE. Membrane translocation of ElmoE or C-terminal ElmoE did not occur in cells that were treated with Latrunculin, suggesting that the actin cytoskeleton is required for signal feedback to enhance the localization of ElmoE.

Elmo and Dock180 form a complex that serves as a GEF for Rac proteins in metazoans (Brugnera et al., 2002; Côté and Vuori, 2007). There are eight genes that encode Dock-like proteins in *D. discoideum* (Meller et al., 2005). We showed that ElmoE associates with the Dock-related proteins DdDockC and DdzizA but not the other five Dock-like proteins (DdDockA is yet to be examined). A previous study showed that ElmoA associates with DdDockD (Para et al., 2009). Thus, it is increasingly clear that Elmo proteins and their Dock-like partners in *D. discoideum* form evolutionarily conserved complexes as they do in higher eukaryotes. Our results show that ElmoE is required for cAR1-induced activation of RacB and proteomic and functional analyses suggest that ElmoE specifically interacts with RacB but not any other of the 17 Rac-like proteins present in *D. discoideum.* Together our data suggests that ElmoE and the Dock-related proteins DdDockC and/or DdzizA may form an evolutionarily conserved Elmo/Dock complex to serve as a GEF for the small G protein RacB.

Our study has provided evidence to suggest that the ElmoE pathway may spatially direct the growth of the dendritic actin network in pseudopods during chemotaxis. Cells lacking ElmoE displayed defects in chemotaxis similar to what was previously shown in *racB*$^-$ cells (Park et al., 2004). In addition, *elmoE*$^-$ and *racB*$^-$ cells displayed a similar reduced level of cAMP-triggered actin polymerization, consistent with ElmoE and RacB functioning in the same pathway to promote actin polymerization. In chemotaxing cells, ElmoE was enriched at the base of the forward-extending F-actin network in leading pseudopods where the Arp2/3 complex also accumulates. Because we do not yet have a specific fluorescence probe for the active form of RacB, we imaged the distribution of RacB-GFP, which reflects both active and inactive forms of the protein, and found that the RacB-GFP signals were uniformly distributed in cytosol in chemotaxing cells. We postulate that localized ElmoE may spatially control/activate RacB predominantly at the leading pseudopod to promote the forward extension of actin network for cell migration. Interestingly, *D. discoideum* ElmoA, in contrast to ElmoE, was found to associate with actin/myosinII to prevent excessive F-actin polymerization around the cell periphery and was excluded from leading pseudopods in chemotaxing cells (Isik et al., 2008), indicating that Elmo proteins function differentially to control chemotaxis.

It has been shown in *D. discoideum* that RacB activates PAKc. PAK proteins are a highly conserved family of protein kinase

regulated by Rac in all eukaryotes (Li et al., 2003; Park et al., 2004). In mammalian cells, it has been suggested that members of the PAK family act on cytoskeletal regulators such as Filamin, LIMK and MLCK (myosin light chain kinase) to control the reorganization of the actin network independent of the Arp2/3 complex (Hofmann et al., 2004). Also in mammals, Rac proteins can coordinate the formation of new actin filaments in an Arp2/3-dependent manner through the SCAR/WAVE complex (Sun et al., 2007). While we do not have direct evidence for RacB regulation of WASP/SCAR activity in *D. discoideum*, our proteomic analyses indicate that ElmoE associates with RacB and the Arp2/3 complex (Figure 3), suggesting that similar pathways are conserved. The pathway, consisting of a GPCR, Gβγ, an ElmoE, Dock-related proteins, and RacB proteins, functions in concert with other pathways, such as PI3K, PLA2, TORC2, (Cai et al., 2010; Charest et al., 2010; Chen et al., 2007; Dong et al., 2005; Li et al., 2003; Liu et al., 2010; Veltman et al., 2008; Weiner et al., 2006) that transduce signals from a GPCR to the actin-network during cell migration in *D. discoideum*. Future studies will reveal whether the molecular mechanism involving the direct interaction between G protein subunits and Elmo/Dock complexes is also conserved in other eukaryotes, and how this pathway mediates chemokine GPCR-controlled cell migrations of mammalian cells.

EXPERIMENTAL PROCEDURES

Chemotaxis Assays

Micropipette Chemotaxis Assay

As previously described, wild-type, *elmoE*$^-$, and *elmoEKI* cells were developed to the chemotactic stage. Cells were plated in a 1-well chamber (Nalge Nunc International, Naperville, IL) and imaged with a Zeiss Laser Scanning Microscope, LSM 510 META, with a 40×, 1.3 NA Plan-Neofluar objective lens. A chemoattractant gradient was generated with a microinjector (Eppendorf, Hamburg, Germany) connected to a micropipette filled with 1 μM cAMP. Cell migration was recorded at 10 s intervals. Computer analysis was performed using DIAS software (Wessels et al., 1998). The generation and measurement of applied cAMP gradient using Alexa 594 fluorescent dye has been previously described in detail (Meier-Schellersheim et al., 2006).

EZ-TAXIScan Chemotaxis Assay

Cell migration was recorded at 15 s intervals at room temperature for 30 min in the EZ-TAXIScan chamber (Effector Cell Institute, Tokyo, Japan), which was assembled as described by the manufacturer. Coverslips and chips used in the chamber were coated with 1% BSA at room temperature for 1 hr. A stable, broad cAMP gradient (0–0.5 μM) was established for the assay. Cell migration analysis was performed with MATLAB software, and has been previously described (Liu et al., 2010).

ElmoE Membrane Translocation upon cAMP Stimulation

Differentiated cells expressing ElmoE-YFP were plated in 4-well chambers (Nalge Nunc International, Naperville, IL) in a volume of 400 μl DB buffer and were stimulated at the indicated concentrations of cAMP by applying a 100 μl volume of cAMP into the well. The temporal-spatial intensity changes of ElmoE-YFP in cells were directly imaged using a confocal microscope.

FRET

The dynamics of Gβ and ElmoE protein interaction upon uniform cAMP stimulation was carried out by using a sensitized emission FRET imaging method (N-FRET) on a Zeiss 710 LSM confocal microscope using a EC plan-Neofluar 40× oil lens (Brzostowski et al., 2009b). Cells expressing Gβ-CFP or ElmoE-YFP alone, Gβ -CFP with ElmoE-YFP, and cAR1-CFP with ElmoE-YFP were differentiated to the chemotactic stage, and stimulated as above. The cells were imaged in three channels: CFP (donor), FRET, and YFP (acceptor) with the following settings: a 449–501 nm band pass was used to collect donor and 524–582 nm band pass was used to collect FRET emissions after excitation with a 440 nm laser. A 524–582 nm band pass was used to collect acceptor emissions after excitation with a 514 nm laser.

Identification of Proteins That Interact with ElmoE

Cells expressing pDV-ElmoE-YFP-TAP were developed to the chemotactic stage. Cells transformed with an empty pDV-CYFP-CTAP vector served as a control. After development with cAMP pulses, cells were washed, resuspended to 4 × 10^7 cells/ml in DB, and shaken with 2 mM caffeine at 200 rpm for 20 min to inhibit endogenous cAMP signaling to bring intracellular responses to basal levels (Brenner and Thoms, 1984). Cells were then stimulated with 50 μM cAMP and an aliquot was removed at 5 s. Cells were lysed in precooled lysis buffer (150 mM NaCl, 1% Triton X-100, 50 mM Tris HCl, pH8.0) containing protease inhibitors (Roche, Chicago, IL). Immunoprecipitation was performed by using the μMACS GFP isolation kit (Miltenyi Biotec, Auburn, CA) according to the manufacturer's protocol. Briefly, cleared lysates were obtained by centrifugation at 10,000 × g for 10 min at 4°C. For immunoprecipitation of ElmoE-YFP, lysates were incubated with μMACS anti-GFP MicroBeads at 4°C for 30 min. After the labeling incubation, the cell lysate was applied onto a μColumn and washed with wash buffer (150 mM NaCl, 1% Igepal CA-630, 0.5% sodium deoxycholate, 0.1% SDS, 50 mM Tris HCl, pH 8.0). Proteins were eluted with Elution Buffer (50 mM Tris HCl, pH 6.8, 50 mM DTT, 1% SDS, 1 mM EDTA, 0.005% bromphenol blue, 10% glycerol) and subjected to SDS-PAGE. Protein bands stained with Coomassie blue were excised for mass spectrometry analysis.

Protein identification work was carried out using NanoLC-MS/MS peptide sequencing technology. In brief, each protein band was destained, cleaned, and digested in-gel with sequencing grade modified trypsin (Promega, Madison, WI). The resulting peptide mixture was analyzed by LC-MS/MS, where a high pressure liquid chromatography instrument with a 75 μm inner diameter reverse phase C18 column was on-line coupled with an ion trap mass spectrometer (Thermo, Palo Alto, CA). The mass spectrometric data acquired were used to search the most recent nonredundant protein database. A specific search was done for the *D. discoideum* database (http://www.dictybase.org).

Coimmunoprecipitation

ElmoE and Gβ

Cells expressing ElmoE-YFP were developed to the chemotactic stage, collected by centrifugation and resuspended in ice-cold buffer (20 mM Tris pH 7.5, 150 mM NaCl) at 7 × 10^7 cells/ml. After stimulation with 50 μM cAMP an aliquot was removed at 5 s. Cells were lysed by adding an equal volume of cold lysis buffer (20 mM Tris pH 7.5, 150 mM NaCl, 0.1% Triton X-100) containing a protease inhibitor cocktail (Roche, Chicago, IL). The lysate was precleared by centrifugation. For coimmunoprecipitations, the precleared lysates were incubated with an anti-GFP polyclonal antibody (Clontech Laboratories, Mountain View, CA) for 90 min, and the immunocomplex was captured by incubating with Protein A/G PLUS-Agarose (Santa Cruz Biotechnology, Santa Cruz, CA) for 2 hr. Immunoprecipitates were separated by SDS-PAGE, and western blot analysis was performed with anti-GFP monoclonal antibody or anti-Gβ polyclonal antibody. As a negative control, wild-type cells were used.

For the reciprocal experiments, precleared lysates of cells coexpressing ElmoE-YFP and His-S-HA-Gβ were incubated with anti-HA MicroBeads. Immunoprecipitation was performed as described above. The eluted proteins were separated by SDS-PAGE, blotted onto a PVDF membrane, and probed with anti-GFP antibody or anti-HA monoclonal antibody. As negative controls, cells expressing ElmoE-YFP and His-S-HA-CRAC, or His-S-HA-PH_{CRAC} were used.

ElmoE, N-ElmoE, C-ElmoE, and Gβ

Cells expressing ElmoE-YFP, N-ElmoE-YFP, or C-ElmoE-YFP were developed and stimulated as above. Precleared lysates of cells were incubated with anti-GFP MicroBeads. Immunoprecipitation was performed as described above. The eluted proteins were separated by SDS-PAGE, and probed with anti-GFP antibody or anti-Gβ polyclonal antibody.

ElmoE and GβSNs

Cells coexpressing ElmoE-YFP and GST-tagged mutant Gβ were developed and stimulated as above. Precleared lysates of cells were incubated with

anti-GST MicroBeads. Immunoprecipitation was performed as described above. The eluted proteins were separated by SDS-PAGE, and probed with anti-GFP antibody or anti-GST antibody.

ElmoE and RacB

Cells coexpressing ElmoE-YFP and myc-RacB were developed and stimulated with or without 10 μM cAMP. Cells coexpressing PH-GFP and myc-RacB were used as a control. Immunoprecipitation was performed by using μMACS GFP isolation kit as described above. Immunoprecipitated proteins were subjected to SDS-PAGE and analyzed by western blot with an anti-myc antibody (Abcam, Cambridge, MA). For the reciprocal experiments, μMACS anti-c-*myc* MicroBeads was used to pull down myc-RacB. ElmoE-YFP was probed for with an anti-GFP antibody (Clontech Laboratories) on western blots.

ElmoE and Dock-like Proteins

Cells coexpressing ElmoE-YFP and GST-tagged or His-S-HA-tagged Dock-like proteins were developed and stimulated as above. Precleared lysates of cells were incubated with anti-GST or anti-HA MicroBeads. Immunoprecipitation was performed as described above. The eluted proteins were separated by SDS-PAGE, and probed with anti-GST, anti-HA, and anti-GFP.

Immunoprecipitation of Membrane Fraction

Cells coexpressing His-S-HA-Gβ and ElmoE-YFP, N-ElmoE-YFP, or C-ElmoE-YFP were developed to the chemotactic stage. After basalation in 2 mM caffeine for 30 min, cells were stimulated with 10 μM cAMP. Aliquots of cells were taken and syringe lysed at indicated time points. The membrane fraction was isolated by centrifugation at 13,000 rpm for 1 min. The supernatant was removed and the pellet was resuspended in Lysis buffer. Immunoprecipitations were carried out as above with anti-HA MicroBeads. The elution was subjected to SDS-PAGE and western blot analysis with an anti-HA or anti-GFP antibody.

Crosslinking Assay

Cells expressing His-S-HA-Gβ were developed, stimulated as described above, and lysed by adding an equal volume of cold lysis buffer (50 mM Na_2HPO_4, 50 mM Na_2HPO_4 [pH 9.5], 0.5% [vol/vol] Triton X-100, EDTA-free protease inhibitor cocktail tablets [Roche, Chicago, IL]), 200 mmol HBVS (Pierce, Rockford, IL). The crosslinking reaction was incubated at room temperature for 5 min and then stopped by adding a 20-fold molar excess of DTT. The crosslinked lysate was precleared by centrifugation and the supernatant was then subjected to tandem affinity purification. First, Ni-NTA agarose chromatography was used to capture the protein via its His tag. The lysate was incubated with Ni-NTA agarose (QIAGEN) for 90 min, followed by a series of washes with 20 mM Tris (pH 8.0), 150 mM NaCl, 0.1% (vol/vol) Triton X-100, containing 20 mM and then 50 mM imidazole. Elution was performed with 20 mM Tris (pH 8.0), 150 mM NaCl, 0.1% (vol/vol) Triton X-100, and 500 mM imidazole. The eluate was diluted with 20 mM Tris (pH 7.5), 150 mM NaCl, to a final concentration of 50 mM imidazole. Next, Triton X-100 was added to 0.01% (vol/vol) and the sample was subjected to S-tag purification by binding to S-protein agarose (Novagen, Madison, WI) for 3 hr followed by a series of washes with 50 mM Tris, (pH 8.0), 0.5 mM EDTA. The elution was performed with 50U AcTEV protease (Invitrogen, Carlsbad, CA) to remove S-protein agarose. Finally, the eluted protein complexes were subjected to mass spectrometry for protein identification.

Rac Activation Assay

The Rac activation assay was performed by affinity precipitation following the protocol in the Rac1 Activation Assay Biochem Kit (Cytoskeleton, Denver, CO) with modifications: Active Rac (Rac-GTP) was isolated with GST-Sepharose beads coupled with PAK (p21 activated kinase 1)-PBD (p21 Binding Domain). Briefly, cells expressing myc-RacB, GFP-RacD, or GFP-RacI (Mondal et al., 2007) were developed, stimulated as described above, and lysed with lysis buffer containing protease inhibitors (Roche). Cleared lysates were obtained by centrifugation at 10,000 rpm, 4°C for 2 min. Lysates were incubated with PAK-PBD beads with rotation at 4°C for 1 hr. The beads were pelleted by centrifugation at 5,000 × g at 4°C for 3 min, washed with wash buffer, and suspended with Laemmli sample buffer and boiled for 2 min. The samples were subjected to SDS-PAGE and western blot analysis with an anti-myc or anti-GFP antibody. The band intensity was quantified with the ImageJ. The levels of Rac-GTP in cells without cAMP stimulation were set at 1.0.

In Vivo Actin Polymerization

The actin in vivo polymerization was determined as described (Shu et al., 2010). Briefly, wild-type and *elmoE*$^-$ cells were developed to chemotactic stage. Cells were harvested, washed with PB and resuspended (3×10^7 cells/ml) in 10 mM PM (PB containing 2 mM $MgSO_4$), and 3 mM caffeine. Cells were stimulated with 1 μM cAMP, fixed and stained in buffer containing 3.7% formaldehyde, 0.15% Triton X-100, 250 nM TRITC-phalloidin, 20 mM KCl, 10 mM Pipes, 5 mM EGTA, and 2 mM MgCl2, pH 6.8. F-actin was quantified by measuring TRITC-phalloidin fluorescence with a LS55 Luminescence spectrometer.

SUPPLEMENTAL INFORMATION

Supplemental Information includes seven figures, one table, Supplemental Experimental Procedures, and two movies and can be found with this article online at doi:10.1016/j.devcel.2011.11.007.

ACKNOWLEDGMENTS

This study was supported by NIAID/NIH and NCI/NIH intramural funds. We thank the members of the Jin lab, and P. Kriebel of the Parent lab. We thank Dicty Stock Center for providing *rasC*$^-$*&rasG*$^-$ strain and plasmids pDV-CYFP-CTAP, pDM314, pDXA-GST, pDXA-GFPABD120, and GFP-Arp2/pBIG; A. Muller-Taubenberger for the ΔlimE-RFP plasmid; M. Dubin and W. Nellen for the vector pDbsrXP6xMYC; F. Rivero for GFP-Racs; M. Zhao at NIAID; and S. Shu and X. Liu at NHLBI/NIH for their technical assistance. We thank X. Xiang for critical comments.

Received: October 27, 2010
Revised: October 19, 2011
Accepted: November 15, 2011
Published online: January 17, 2012

REFERENCES

Bosgraaf, L., and van Haastert, P.J. (2006). The regulation of myosin II in Dictyostelium. Eur. J. Cell Biol. *85*, 969–979.

Brenner, M., and Thoms, S.D. (1984). Caffeine blocks activation of cyclic AMP synthesis in Dictyostelium discoideum. Dev. Biol. *101*, 136–146.

Bretschneider, T., Diez, S., Anderson, K., Heuser, J., Clarke, M., Müller-Taubenberger, A., Köhler, J., and Gerisch, G. (2004). Dynamic actin patterns and Arp2/3 assembly at the substrate-attached surface of motile cells. Curr. Biol. *14*, 1–10.

Brugnera, E., Haney, L., Grimsley, C., Lu, M., Walk, S.F., Tosello-Trampont, A.C., Macara, I.G., Madhani, H., Fink, G.R., and Ravichandran, K.S. (2002). Unconventional Rac-GEF activity is mediated through the Dock180-ELMO complex. Nat. Cell Biol. *4*, 574–582.

Brzostowski, J.A., Fey, P., Yan, J., Isik, N., and Jin, T. (2009a). The Elmo family forms an ancient group of actin-regulating proteins. Commun. Integr. Biol. *2*, 337–340.

Brzostowski, J.A., Meckel, T., Hong, J., Chen, A., and Jin, T. (2009b). Imaging protein-protein interactions by Forster resonance energy transfer (FRET) microscopy in live cells. Curr. Protoc. Protein Sci. *Chapter 19*, Unit19 15.

Cai, H., Das, S., Kamimura, Y., Long, Y., Parent, C.A., and Devreotes, P.N. (2010). Ras-mediated activation of the TORC2-PKB pathway is critical for chemotaxis. J. Cell Biol. *190*, 233–245.

Charest, P.G., Shen, Z., Lakoduk, A., Sasaki, A.T., Briggs, S.P., and Firtel, R.A. (2010). A Ras signaling complex controls the RasC-TORC2 pathway and directed cell migration. Dev. Cell *18*, 737–749.

Chen, L., Iijima, M., Tang, M., Landree, M.A., Huang, Y.E., Xiong, Y., Iglesias, P.A., and Devreotes, P.N. (2007). PLA2 and PI3K/PTEN pathways act in parallel to mediate chemotaxis. Dev. Cell *12*, 603–614.

Chen, M.Y., Long, Y., and Devreotes, P.N. (1997). A novel cytosolic regulator, Pianissimo, is required for chemoattractant receptor and G protein-mediated activation of the 12 transmembrane domain adenylyl cyclase in Dictyostelium. Genes Dev. *11*, 3218–3231.

Côté, J.F., and Vuori, K. (2007). GEF what? Dock180 and related proteins help Rac to polarize cells in new ways. Trends Cell Biol. *17*, 383–393.

Côté, J.F., Motoyama, A.B., Bush, J.A., and Vuori, K. (2005). A novel and evolutionarily conserved PtdIns(3,4,5)P3-binding domain is necessary for DOCK180 signalling. Nat. Cell Biol. *7*, 797–807.

Dong, X., Mo, Z., Bokoch, G., Guo, C., Li, Z., and Wu, D. (2005). P-Rex1 is a primary Rac2 guanine nucleotide exchange factor in mouse neutrophils. Curr. Biol. *15*, 1874–1879.

Dupré, D.J., Robitaille, M., Rebois, R.V., and Hébert, T.E. (2009). The role of Gbetagamma subunits in the organization, assembly, and function of GPCR signaling complexes. Annu. Rev. Pharmacol. Toxicol. *49*, 31–56.

Funamoto, S., Meili, R., Lee, S., Parry, L., and Firtel, R.A. (2002). Spatial and temporal regulation of 3-phosphoinositides by PI 3-kinase and PTEN mediates chemotaxis. Cell *109*, 611–623.

Futrelle, R.P., Traut, J., and McKee, W.G. (1982). Cell behavior in Dictyostelium discoideum: preaggregation response to localized cyclic AMP pulses. J. Cell Biol. *92*, 807–821.

Hadwiger, J.A., and Firtel, R.A. (1992). Analysis of G alpha 4, a G-protein subunit required for multicellular development in Dictyostelium. Genes Dev. *6*, 38–49.

Hofmann, C., Shepelev, M., and Chernoff, J. (2004). The genetics of Pak. J. Cell Sci. *117*, 4343–4354.

Iijima, M., and Devreotes, P. (2002). Tumor suppressor PTEN mediates sensing of chemoattractant gradients. Cell *109*, 599–610.

Iijima, M., Huang, Y.E., and Devreotes, P. (2002). Temporal and spatial regulation of chemotaxis. Dev. Cell *3*, 469–478.

Insall, R., Kuspa, A., Lilly, P.J., Shaulsky, G., Levin, L.R., Loomis, W.F., and Devreotes, P. (1994). CRAC, a cytosolic protein containing a Pleckstrin homology domain, is required for receptor and G protein-mediated activation of adenylyl cyclase in Dictyostelium. J. Cell Biol. *126*, 1537–1545.

Insall, R.H., and Machesky, L.M. (2009). Actin dynamics at the leading edge: from simple machinery to complex networks. Dev. Cell *17*, 310–322.

Isik, N., Brzostowski, J.A., and Jin, T. (2008). An Elmo-like protein associated with myosin II restricts spurious F-actin events to coordinate phagocytosis and chemotaxis. Dev. Cell *15*, 590–602.

Janetopoulos, C., Jin, T., and Devreotes, P. (2001). Receptor-mediated activation of heterotrimeric G-proteins in living cells. Science *291*, 2408–2411.

Jin, T., Amzel, M., Devreotes, P.N., and Wu, L. (1998). Selection of gbeta subunits with point mutations that fail to activate specific signaling pathways in vivo: dissecting cellular responses mediated by a heterotrimeric G protein in Dictyostelium discoideum. Mol. Biol. Cell *9*, 2949–2961.

Jin, T., Zhang, N., Long, Y., Parent, C.A., and Devreotes, P.N. (2000). Localization of the G protein betagamma complex in living cells during chemotaxis. Science *287*, 1034–1036.

Jin, T., Xu, X., and Hereld, D. (2008). Chemotaxis, chemokine receptors and human disease. Cytokine *44*, 1–8.

Kimmel, A.R., and Parent, C.A. (2003). The signal to move: D. discoideum go orienteering. Science *300*, 1525–1527.

Li, Z., Hannigan, M., Mo, Z., Liu, B., Lu, W., Wu, Y., Smrcka, A.V., Wu, G., Li, L., Liu, M., et al. (2003). Directional sensing requires G beta gamma-mediated PAK1 and PIX alpha-dependent activation of Cdc42. Cell *114*, 215–227.

Liu, L., Das, S., Losert, W., and Parent, C.A. (2010). mTORC2 regulates neutrophil chemotaxis in a cAMP- and RhoA-dependent fashion. Dev. Cell *19*, 845–857.

Meier-Schellersheim, M., Xu, X., Angermann, B., Kunkel, E.J., Jin, T., and Germain, R.N. (2006). Key role of local regulation in chemosensing revealed by a new molecular interaction-based modeling method. PLoS Comput. Biol. *2*, e82.

Meller, N., Merlot, S., and Guda, C. (2005). CZH proteins: a new family of Rho-GEFs. J. Cell Sci. *118*, 4937–4946.

Mondal, S., Neelamegan, D., Rivero, F., and Noegel, A.A. (2007). GxcDD, a putative RacGEF, is involved in Dictyostelium development. BMC Cell Biol. *8*, 23.

Para, A., Krischke, M., Merlot, S., Shen, Z., Oberholzer, M., Lee, S., Briggs, S., and Firtel, R.A. (2009). Dictyostelium Dock180-related RacGEFs regulate the actin cytoskeleton during cell motility. Mol. Biol. Cell *20*, 699–707.

Parent, C.A., and Devreotes, P.N. (1999). A cell's sense of direction. Science *284*, 765–770.

Parent, C.A., Blacklock, B.J., Froehlich, W.M., Murphy, D.B., and Devreotes, P.N. (1998). G protein signaling events are activated at the leading edge of chemotactic cells. Cell *95*, 81–91.

Park, K.C., Rivero, F., Meili, R., Lee, S., Apone, F., and Firtel, R.A. (2004). Rac regulation of chemotaxis and morphogenesis in Dictyostelium. EMBO J. *23*, 4177–4189.

Pollard, T.D., and Borisy, G.G. (2003). Cellular motility driven by assembly and disassembly of actin filaments. Cell *112*, 453–465.

Reddien, P.W., and Horvitz, H.R. (2004). The engulfment process of programmed cell death in Caenorhabditis elegans. Annu. Rev. Cell Dev. Biol. *20*, 193–221.

Shu, S., Liu, X., Kriebel, P.W., Hong, M.S., Daniels, M.P., Parent, C.A., and Korn, E.D. (2010). Expression of Y53A-actin in Dictyostelium disrupts the cytoskeleton and inhibits intracellular and intercellular chemotactic signaling. J. Biol. Chem. *285*, 27713–27725.

Sun, C.X., Magalhães, M.A., and Glogauer, M. (2007). Rac1 and Rac2 differentially regulate actin free barbed end formation downstream of the fMLP receptor. J. Cell Biol. *179*, 239–245.

Van Haastert, P.J., and Devreotes, P.N. (2004). Chemotaxis: signalling the way forward. Nat. Rev. Mol. Cell Biol. *5*, 626–634.

Veltman, D.M., Keizer-Gunnik, I., and Van Haastert, P.J. (2008). Four key signaling pathways mediating chemotaxis in Dictyostelium discoideum. J. Cell Biol. *180*, 747–753.

Vlahou, G., and Rivero, F. (2006). Rho GTPase signaling in Dictyostelium discoideum: insights from the genome. Eur. J. Cell Biol. *85*, 947–959.

Weiner, O.D., Rentel, M.C., Ott, A., Brown, G.E., Jedrychowski, M., Yaffe, M.B., Gygi, S.P., Cantley, L.C., Bourne, H.R., and Kirschner, M.W. (2006). Hem-1 complexes are essential for Rac activation, actin polymerization, and myosin regulation during neutrophil chemotaxis. PLoS Biol. *4*, e38.

Wessels, D., Voss, E., Von Bergen, N., Burns, R., Stites, J., and Soll, D.R. (1998). A computer-assisted system for reconstructing and interpreting the dynamic three-dimensional relationships of the outer surface, nucleus and pseudopods of crawling cells. Cell Motil. Cytoskeleton *41*, 225–246.

Wu, L., Valkema, R., Van Haastert, P.J., and Devreotes, P.N. (1995). The G protein beta subunit is essential for multiple responses to chemoattractants in Dictyostelium. J. Cell Biol. *129*, 1667–1675.

Xu, X., Meier-Schellersheim, M., Jiao, X., Nelson, L.E., and Jin, T. (2005). Quantitative imaging of single live cells reveals spatiotemporal dynamics of multistep signaling events of chemoattractant gradient sensing in Dictyostelium. Mol. Biol. Cell *16*, 676–688.

Xu, X., Meier-Schellersheim, M., Yan, J., and Jin, T. (2007). Locally controlled inhibitory mechanisms are involved in eukaryotic GPCR-mediated chemosensing. J. Cell Biol. *178*, 141–153.

Xu, X., Meckel, T., Brzostowski, J.A., Yan, J., Meier-Schellersheim, M., and Jin, T. (2010). Coupling mechanism of a GPCR and a heterotrimeric G protein during chemoattractant gradient sensing in Dictyostelium. Sci. Signal. *3*, ra71.

Zhang, N., Long, Y., and Devreotes, P.N. (2001). Ggamma in dictyostelium: its role in localization of gbetagamma to the membrane is required for chemotaxis in shallow gradients. Mol. Biol. Cell *12*, 3204–3213.